June 1992 | Interim

A Study of Supermaneuverable Flight Trajectories Through Motion Field Simulation of a Centrifuge Simulator

PE - 62202F
PR - 7231
TA - 723125
WU - 72312502

D.W. Repperger

Armstrong Laboratory, Crew Systems Directorate
Biodynamics and Biocommunications Division
Human Systems Center
Air Force Materiel Command
Wright-Patterson AFB OH 45433-7008

AL-TR-1993-0037

Published in Transactions of the ASME Journal of Dynamic Systems, Measurement, and Control

The advent of supermaneuverable flight trajectories for high performance aircraft opens up new research areas involving the human factors effects on pilots when they fly these unusual flight scenarios. There exists a need to conduct studies in motion simulators such as centrifuges to investigate how these unusual motion fields effect humans both physiologically and how they impact the ability of a pilot to perform a mission. The dynamic control of a centrifuge simulator to emulate supermaneuverable flight trajectories is studied in this paper by considering the centrifuge simulator as a 3 revolute axes robot manipulator.

Supermaneuverability, Motion Simulation, Robotic Manipulator | 8

Unclassified | Unclassified | Unclassified | Unlimited

A Study of Supermaneuverable Flight Trajectories Through Motion Field Simulation of a Centrifuge Simulator

D. W. Repperger
Armstrong Laboratory/CFBS,
Wright Patterson Air Force Base,
Dayton, Ohio 45433-6573

The advent of supermaneuverable flight trajectories for high performance aircraft opens up new research areas involving the human factors effects on pilots when they fly these unusual flight scenarios. There exists a need to conduct studies in motion simulators such as centrifuges to investigate how these unusual motion fields effect humans both physiologically and how they impact the ability of a pilot to perform a mission. The dynamic control of a centrifuge simulator to emulate supermaneuverable flight trajectories is studied in this paper by considering the centrifuge simulator as a 3 revolute axes robot manipulator.

Introduction

Supermaneuverability (Clark, 1987; Cook, 1989; Cord, 1990; Hague, 1981; Schefter, 1989; Sweetman, 1990) refers to the unusual flight trajectories presently being investigated with high performance fighter aircraft. Present fighters can be made to fly these unusual flight maneuvers by several known methods: using a high angle of attack ($\alpha > 50$ degrees), thrust vectoring, vortex manipulation for control, or possibly using differential deflection of stabilizers or canards. Most supermaneuverable flight trajectories have not actually been flown in aircraft but studies with 1/7 th. size prototypes are presently being conducted to investigate structural problems and the measurement of the linear and rotational accelerations and forces that would act on a pilot (Gal-Or, 1990) during a specified maneuver. In his work a set of all pitch and roll angles of a specified aircraft (F-15) were determined where both controllable and stable flight will occur. This region of aircraft attitude is clearly a function of both the altitude and speed due to the structural problems and controllability issues associated with flying an aircraft in this unusual regime.

One particularly well-known supermaneuver is the "Cobra Maneuver" which has been recently flown at airshows (*Aviation Week*, 1990) by both Soviet and U.S. high performance aircraft. Recent work (Chiang et al., 1990) has addressed the problem of controller design in these unusual flight scenarios in which there exists a compromise of high angle of attack to controllability and stability. In their study an FA/18 was utilized because of its use of thrust vectoring as a procedure to produce the supermaneuver. Their motivation was based on a previous study (Kalviste, 1986) in which it was shown that a pilot *must control* both the standard P and Q angles simultaneously to change the aircraft's body axis roll angle. This is because neither the body X-axis nor the velocity vector (wing X-axis) can be used as the roll-axis reference. Both these variables change directions, themselves, during the supermaneuver.

One main issue which has not been addressed is how such unusual flight scenarios will affect pilots in their ability to continue to perform tasks during the mission. To understand better these human factors issues, it is necessary to conduct research with pilots on a ground based motion simulator that will reasonably replicate the motion field experienced by pilots flying these unusual maneuvers. The term "reasonably replicate" is mathematically formulated in this paper using a Damped Least Squares numerical procedure. A motion simulator (large centrifuge) exists at Wright Patterson Air Force Base, Dayton, Ohio in the form of a large three-degree-of-freedom device which is used to test pilots and equipment. The analysis of its control to produce trajectories to emulate supemaneuverable aircraft will be conducted in this study by analyzing the centrifuge simulator within the context of a large robot.

A centrifuge simulator differs from traditional robots because of three fundamental reasons. First, its size is prohibitively large (190 tons in weight and 25 feet in height) but it can be considered a robot with 3 revolute joints (all axes have 360 degrees of rotation). Second, the centrifuge has a simplification (due to balancing conditions) of having the same dynamic payload at all points during its dynamic operation (the inertia-mass matrix is constant for all time) This is a great aid in simplifying the computations. The third way the centrifuge simulator differs from traditional robots is due to the fact that its goal is to create an unusually different motion field at a particular point on the end effector (at a point on a seat within the centrifuge). This motion field will consist of a specified linear acceleration (a three-dimensional vector) which changes

Contributed by the Dynamics Systems and Control Division for publication in the JOURNAL OF DYNAMIC SYSTEMS, MEASUREMENT, AND CONTROL. Manuscript received by the Dynamic Systems and Control Division January 1991; revised manuscript received September 3, 1991. Associate Technical Editor: H. Kazerooni.

as a function of time and also a particular rotational motion field of a fixed coordinate system at the rigid body defined at the endpoint on the seat of the centrifuge where the pilot is located. This rotational motion field may also vary as a function of time. The study of this type of problem differs from the traditional control theory approaches in robotics where it is desired to control the position of the end effector or the force at the end effector in contact with the environment. First it is necessary to formulate the problem of interest as it applies to a centrifuge simulator.

Formulation of the Problem of Interest

Let X be a 3×1 position vector in Cartesian space and θ a 3×1 joint space vector. The forward kinematics relationship between X and θ can be specified via:

$$X = f(\theta) \tag{1}$$

where the function $f(.)$ (cf. Repperger, 1990) for a centrifuge motion simulator is an extremely complicated function of the 3 joint variables $\theta_i(t)$, $(i = 1, 3)$. If X is a linear position vector and denoting its 3×1 dimensional velocity vector as V, then:

$$V = \dot{X} = J1\dot{\theta} \tag{2}$$

as the linear velocity relationship and the dot indicates time differentiation. $J1$ is the 3×3 Jacobian matrix associated with linear velocities.

If the vector Ω represents the angular velocity of a coordinate frame located at the end effector within the simulator, then the representation:

$$\Omega = J2\dot{\theta} \tag{3}$$

is derived in detail in the sequel. Here $J2$ is another 3×3 Jacobian matrix associated with rotational velocities. Combining equations (2,3), it is seen that:

$$\text{col}\,[V,\Omega] = \text{col}[J1, J2]\dot{\theta} = J\dot{\theta} \tag{4}$$

where J is defined as the overall 6×3 Jacobian for this system. J can be calculated in a variety of ways (see Orin and Schrader, 1984) and in the sequel one method to calculate this matrix is presented for the centrifuge from the forward kinematic equations.

What is of interest in Air Force applications, however, is the linear accelerations acting on a pilot located at the endpoint of the centrifuge. This motion field produces forces acting on a pilot which physiologically stress him. In addition, it is necessary to separate out the Coriolis accelerations from the centrifugal and gravity terms. The Coriolis accelerations are extremely undesirable in both linear acceleration stress studies and in rotational studies involving spatial disorientation. However, it is necessary to keep careful account of these Coriolis terms due to efforts to dynamically control out these particular terms. To develop the linear acceleration terms, the chain rule is used in differentiating Eq. (2) to yield:

$$a = \dot{V} = J1\ddot{\theta} + \dot{J}1\dot{\theta} \tag{5}$$

where a is the 3×1 acceleration vector and $\dot{J}1$ would be a third order tensor in this notation. The term $\ddot{\theta}$ is used in this context to denote a vector of joint accelerations. Thus to develop the motion field desired within a centrifuge simulator for studies involving man-machine systems, one is particularly interest in the relationships (3) and (5).

What complicates the problem is that the 3×1 vector a on

Nomenclature

α = the angle of attack of an aircraft (pitch angle)

X = the cartesian position vector

$\theta_i (i = 1 = 3)$ = the joint angles of the centrifuge or robot

θ_k = stepwise time integration of the joint vector θ

Δt = time step

V = linear velocity vector

Ji $(i = 1 = ,2)$ = Jacobians of the robot or centrifuge

Ω = angular rotation vector

$\dot{\theta}_i = \omega_i$ = specific joint rotation velocities for joint i $(i = 1,3)$

a = linear acceleration vector

C = a scalar constraint on the joint velocities as a result of a Euclidean norm operation

L = cost functional to weigh both rotational motion artifact and limits on the finite joint velocities allowed

Ri $(i = 1,2)$ = the weighting matrices in the L cost functional

λ = adjoint variable of the cost functional L used to weigh joint velocities

$(r_i)^2$ $(i = 1,2)$ = residual terms of the cost functional. r1 weights motion artifact in rotational space; r2 weights limits on joint velocities

P_i $(i = 0,5)$ = position vectors describing the selection of coordinate frames using the Denavit-Hartenberg formulation

$L1$, $L2$, Lx, Ly, Lz, Lt, θ_t, and θ_y = fixed quantities of the centrifuge simulator including arm and seat lengths and seat rotations to describe the Denavit-Hartenberg parameters in the transformation matrix

(X_i, Y_i, Z_i) $(i = 0,5)$ = describe the coordinate frames selected in the Denavit-Hartenberg transformation

T_i^j = the transformation matrix from frame i to j using the Denavit-Hartenberg formulation

R, $Px1$, $Py1$, $Pz1$ = notation in Denavit-Hartenberg formulation where R represents the rotation matrix, and the P_j $(j = x1, y1, z1)$ are position vectors

i_m, k_m, j_m $(m = 0,5)$ = unit vectors in the mth selected coordinate frame

$Aj(t)$, $Bj(t)$, and $Cj(t)$ $(j = 0,3)$ = coefficient matrices of the unit vectors in the various coordinate frames of interest to describe rotational motion

$\theta x(t)$, $\theta y(t)$, $\theta z(t)$ = actual (body axes) rotations a pilot sees when he sits in the centrifuge simulator or in an actual aircraft during the supermaneuver

$\Omega j(t)$, $(j = x, y, z)$ = actual (body axes) rotational velocities a pilot sees when he sits in the centrifuge simulator or in an actual aircraft

the left-hand side of (5) is specified as a function of time. Simultaneously the 3×1 vector $\Omega(t)$ in (3) is now determined if the θ_i variables in (5) are initially specified by the requirements for $a(t)$. Thus for the simulation of certain motion fields, there exists situations where the problem may be over or under determined and one must be careful to determine if the linear or rotational motion field specified provides a well posed problem for the given simulator. It is necessary to define two problems of interest.

The first problem of interest would be the selection of the joint commands $\theta_i(t)$ such that the linear acceleration vector $a(t)$ at the end effector would match a desired motion trajectory. The second problem would be the selection of the joint commands $\theta_i(t)$ to match the rotational time histories of the coordinate frames located at the end effector to emulate a specified motion field. For simplicity the second problem will be considered in this paper.

For the robotics problem of interest, it is desired to find $\dot{\theta}$ to achieve a particular motion trajectory $\dot{X}(t)$ which is specified apriori. To relate this procedure to a practical problem (Repperger, 1990, 1991) involving motion base simulation of a specified aircraft trajectory on a simulator, we define as the problem of interest (e.g., using only Eq. (3) when J2 is square) to solve for $\dot{\theta}$, when Ω may be specified, i.e.:

$$\dot{\theta} = [J2]^{-1}\Omega \tag{6}$$

If, however, J2 is in a nearly rank deficient configuration, this leads to excessively high joint velocities $\dot{\theta}$. There may exist a practical constraint of the form:

$$\|\dot{\theta}\|^2 \leq C \tag{7}$$

to make such a problem realizable. The norm used in Eq. (7) refers to the standard Euclidean norm.

The Damped Least Squares numerical method provides an ideal way to convert the constraint problem specified by (6-7) into an optimization procedure.

Damped Least Squares

This type of algorithm is ideal when the Jacobian may become nearly singular (Wampler, 1986; Maciejewski and Klein, 1988). To understand how this procedure handles the singularities of the Jacobian, the objective is to minimize L specified by:

$$L = \|\dot{X} - J\dot{\theta}\|^2 + \lambda^2\|\dot{\theta}\|^2 \tag{8}$$

where $\lambda > 0$ is selected to be constant in this paper and to minimize joint velocities if the Jacobian becomes singular. Thus the fidelity of the motion field (denoted by $\|\dot{X} - J\dot{\theta}\|^2$) is compromised by trading off a cost associated with a weighting in $\lambda^2\|\dot{\theta}\|^2$. This is appropriate for a centrifuge simulator in which finite torque on the axes limits the $\dot{\theta}$ values. Also, since the energy in the simulator is proportional to $\dot{\theta}$, this is consistent with the finite energy available to produce motor torques.

By minimizing $\dot{\theta}$ of Eq. (8), this yields the augmented equation:

$$\text{col}[J, \lambda I]\dot{\theta} = \text{col}[\dot{X}, 0] \tag{9}$$

which requires solving:

$$(J^TJ + \lambda^2 I)\dot{\theta} = J^T\dot{X} \tag{10}$$

or

$$\dot{\theta} = (J^TJ + \lambda^2 I)^{-1}J^T\dot{X} \tag{11}$$

as the inverse kinematics solution. Thus if $\lambda = 0$ in Eq. (11), this reduces to the results specified in Eq. (6). This approach easily extends to redundant systems where J may not be square.

To understand how this technique handles the singularities of the Jacobian J2 for the rotational simulation problem, the objective in this case is to minimize L now being specified by:

$$L = \|\Omega - J2\dot{\theta}\|^2_{R1} + \lambda^2\|\dot{\theta}\|^2_{R2} \tag{12}$$

where $\lambda > 0$ is selected to minimize joint velocities if the Jacobian becomes singular. One could rewrite Eq. (12) to analyze each term separately. Denote a residuals term $r1$ and an energy term $r2$ with weighting matrices $R1$ and $R2$ as follows:

$$(r1)^2 = \|\Omega - J2\dot{\theta}\|^2_{R1},\ R1 > 0 \tag{13}$$

$$(r2)^2 = \lambda^2\|\dot{\theta}\|^2_{R2},\ R2 > 0 \tag{14}$$

The Damped Least Squares analogy related to the above problem, involves the selection of $\dot{\theta}$ such that the following relationship is approximately correct:

$$\dot{\theta} \approx [J2]^{-1}\Omega \tag{15}$$

Thus the fidelity of the motion field (denoted by $\|\Omega - J2\dot{\theta}\|^2_{R1}$) is compromised by trading off a cost associated with a weighting in $\lambda^2\|\dot{\theta}\|^2_{R2}$. By minimizing L of Eq. (12) for the rotational motion study, this yields the augmented equation:

$$\text{col}[J2, \lambda I]\dot{\theta} = \text{col}[\Omega, 0] \tag{16}$$

which requires solving:

$$(J2^TJ2 + \lambda^2 I)\dot{\theta} = J2^T\Omega \tag{17}$$

or

$$\dot{\theta} = (J2^TJ2 + \lambda^2 I)^{-1}J2^T\Omega \tag{18}$$

as the inverse kinematics solution for the rotational simulation problem which is similar in form to the linear acceleration case.

This procedure will now be worked with an example from a motion simulation problem on a centrifuge to illustrate the applicability of this approach.

Application of the Approach to a Motion Simulation Problem

The concept of treating a very large motion simulator (centrigue) as a "large robot" leads to some interesting new perspectives on how to dynamically control such a device. In Repperger (1990) it was shown that work volume (or performance volume) plots of such a device can be obtained in linear acceleration space, rotational velocity, and rotational acceleration space. This can be related to an acceleration radius concept (Graettinger and Krogh, 1988) in which a spherical volume figure is obtained which represents the (three dimensional) linear accelerations attainable at the end effector. It is noted that this type of volume is restricted to a spherical figure; the performance volume in (Repperger, 1990), however, is not restricted to any particular geometric shape. Since performance volumes of this type can be determined, the next step in understanding better ways to control this simulator, if a motion trajectory is specified apriori, involves the solution of the inverse kinematics problem. To accomplish this task, the determination of the joint motions is required to emulate a specified path trajectory at some endpoint within the centrifuge. The last step for the control engineer to regulate the motion of this simulator would be to solve the inverse dynamics problem. This involves the calculation of the required torques (or command inputs) at the actuators to produce the complex acceleration field desired at a point of interest within the centrifuge. In this study the required torques are bounded by the variable C in Eq. (7) (and thus the inverse dynamics problem is solved as a consequence of this procedure) using the Damped Least Squares procedure. This method implicitly utilizes the constraint relationship in Eq. (7). First the forward kinematics problem must be formulated to determine the Jacobian J2 and to observe if the motion simulation problem is well posed.

Problem 1 - The Forward Kinematics Problem

Figure 1 illustrates a diagram describing the DES (Dynamic

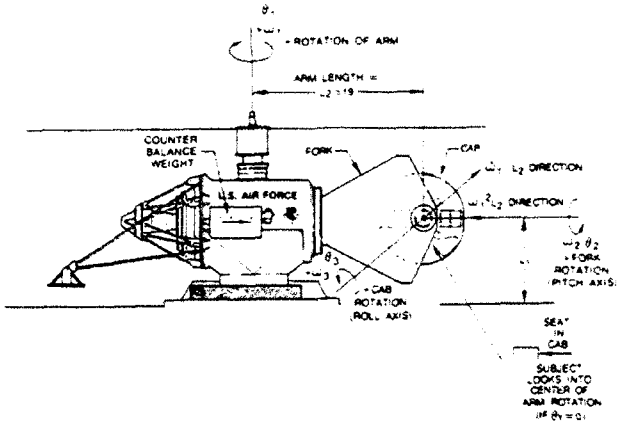

Fig. 1 The DES (Dynamic Environment Simulator)

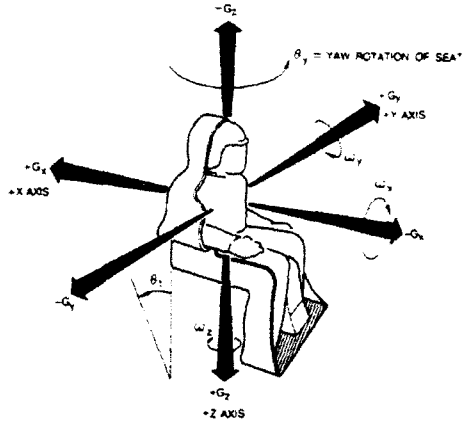

Fig. 2 The body axis coordinate system used for human studies

Environment Simulator). This device is a 19 foot radius centrifuge with the principal axis of rotation (θ_1) as shown in the figure with an angular velocity $\omega_1(t)$. In general the arm rotates clockwise when viewed from the top as indicated in the figure. At the end of the arm is the fork which rotates, using its own control system, about the pitch axis (θ_2). The cab also rotates independently about the same center of rotation as the fork but in the roll axis as illustrated in Fig. 1. The human subject is positioned in the cab as indicated.

Within the cab, at the seat, is illustrated the body centered coordinate system used in acceleration research for human subjects who ride centrifuges (Fig. 2). This includes a yaw rotation of the seat about the body centered $(-z)$ axis (coincident with the vertical axis of the cab), and a seat back angle θ_t. The objective is to calculate the accelerometer readings at point P_5 in Fig. 3 induced by the simulator motion only. Initially the force of gravity is not considered, however, when the forward kinematic chain is determined, the directional cosines of the transformation matrix will indicate the contribution of the gravity vector to the readings of the accelerometers positioned on the seat at point P_5.

In Fig. 3 at the point P_5 of the body centered coordinate system located on the seat displayed in Fig. 2, it is first desired to calculate the linear acceleration experienced with respect to all the variables θ_1, ω_1, $\dot{\omega}_1$, $L1$, $L2$, θ_2, $\dot{\theta}_2$, $\ddot{\theta}_2$, θ_3, $\dot{\theta}_3$, $\ddot{\theta}_3$, Lx, Ly, Lz, Lt, θ_t, and θ_y. It is noted that the variables $L1$, $L2$, (defined in Fig. 1), Lx, Ly, Lz, Lt, θ_t, and θ_y (defined in Fig. 3) are fixed quantities which never change once the simulator motion begins. Table 1 lists the actual values of these fixed variables as they apply to the motion simulator in Fig. 1 with the maximum and minimum values of the rotational variables listed.

To develop the forward kinematic relationships due only to simulator motion, it is required to use 6 coordinate systems.

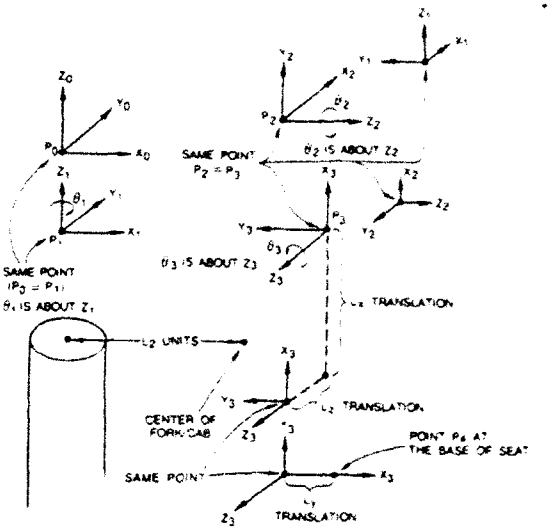

Fig. 3(a)

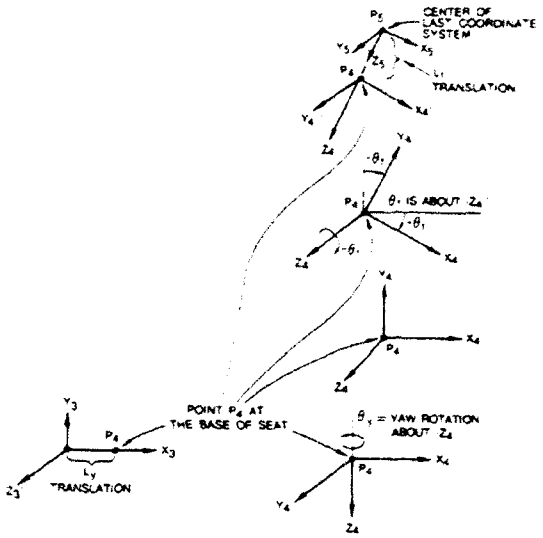

Fig. 3(b)

Fig. 3 The coordinate systems used for the Denavit-Hartenberg formulation of the forward kinematics equations

Let the point P_0 be at the center of the coordinate system (X_0, Y_0, Z_0) and attached to the stationary frame of the centrifuge (the rigid body called the fixed base, (cf. Fig. (3)), the point P_1 is attached to the arm which is also illustrated in Fig. 3 as being the origin of the coordinate system (X_1, Y_1, Z_1) (the second rigid body). The third coordinate system (X_2, Y_2, Z_2) at point P_2 is attached to the fork of the centrifuge at its center of rotation. The fourth coordinate system ((X_3, Y_3, Z_3) at point P_3) is attached to the cab at the same center of rotation of the fork/cab. The point P_4 (with coordinate system (X_4, Y_4, Z_4)) is a translation of $(-Lx, -Ly, Lz)$ units to the bottom the seat (at floor level). The point P_5 is a translation of Lt units up the seat (after the seat is rotated $-\theta_t$ degrees about $-Z_4$") to the point where the accelerometers are mounted. Table 2 illustrates the $D-H$ parameters for the centrifuge simulator.

To determine the Jacobian $J1$ (for the linear stress problem previously introduced), the last coordinate system (cf. Fig. 3) of interest is written (cf. Craig, 1986):

$$\text{col}[X17,\ Y17,\ Z17] = T_0^{17}\,\text{col}[X0,\ Y0,\ Z0] \qquad (19)$$

and T_0^{17} can be expressed:

Table 1 The fixed quantities of the centrifuge simulator

Fixed Variable	Dimensions	Rotational Variable	Max	Min	Dimensions
$L1$	10.4 ft	θ_1	6.28	0	radians
$L2$	19.0 ft	Ω_1	5.86	−5.86	radians/second
Lx	3.3 ft	Ω_1	0.25	−0.25	radians/s/s
Ly	0.1 ft	θ_2	6.28	0	radians
Lz	0.1 ft	Ω_2	3.14	−3.14	radians/second
Lt	2.3 ft	Ω_2	2.5	−2.5	radians/s/s
θ_3	1.57 radians	θ_3	6.28	0	radians
θ_t	.53 radians	Ω_3	3.14	−3.14	radians/second
		Ω_3	5.0	−5.0	radians/s/s

Table 2 The Denavit-Hartenberg parameters for the centrifuge

Link i	Angle From zi-1 to zi about Xi-1 $=ai$-1	Distance Along zi-1 to zi along X'-1 $=Ai$-1	Distance Along Xi-1 to Xi along Zi $=di$	Angle From Xi-1 to Xi about Zi $=\Theta i$
1	0	0	0	$-\theta 1$
2	0	L2	0	0
3	0	0	0	$\pi/2$
4	$+\pi/2$	0	0	0
5	0	0	0	$\theta 2$
6	0	0	0	$+\pi/2$
7	$-\pi/2$	0	0	0
8	0	0	0	$\theta 3$
9	0	−Lx	+Lz	0
10	0	0	0	$-\pi/2$
11	0	Ly	0	0
12	$+\pi/2$	0	0	0
13	0	0	0	$-\theta y$
14	$-\pi/2$	0	0	0
15	0	0	0	$-\theta t$
16	$+\pi/2$	0	0	0
17	0	0	−Lt	0

$$T_0^{17} = \begin{pmatrix} R & Px1 \\ & Py1 \\ \cdots & Pz1 \\ \text{----} & \text{--} \end{pmatrix} \tag{20}$$

where R is the 3×3 rotation matrix. The Jacobian can be expressed:

$$J(\theta)^0 = \begin{pmatrix} \partial Px1/\partial\theta1, & \partial Px1/\partial\theta2, & \partial Px1/\partial\theta3, \\ \theta Py1/\partial\theta1, & \theta Py1/\partial\theta2, & \theta Py1/\partial\theta3, \\ \partial Pz1/\partial\theta1, & \partial Pz1/\partial\theta2, & \partial Pz1/\partial\theta3, \end{pmatrix} \tag{21}$$

The elements of the matrices in Eqs. (20) and (21) are not written out in detail due to their complexity. The derivation, however, is straightforward as described using Eqs. (19)–(21).

Accelerometer Readings Due Only to Gravity

Once the transformation matrix T_0^{17} is derived from the Denavit-Hartenberg parameters describing the centrifuge simulator in Table 2, the linear accelerations due only to gravity can be determined from the directional cosines. To determine these readings, one must find the component of gravity in the final coordinate system with unit vectors (i_5, j_5, k_5). Due to the fact that the T_0^{17} has an orthogonal inverse matrix T_{17}^0, it can easily be shown that the gravity vector produces an acceleration in the last coordinate frame with the following components:

$$i_5\text{component} = -T_{17}^0(3, 1) \tag{22}$$

$$= -s2\ sy\ ct + c2\ c3\ st - c2\ s3\ cy\ ct \tag{23}$$

$$j_5\text{component} = -T_{17}^0(3, 2) \tag{24}$$

$$= -s2\ cy - c2\ s3\ sy \tag{25}$$

$$k_5\text{component} = -T_{17}^0(3, 3) \tag{26}$$

$$= -sy\ st\ s2 + c2\ c3\ ct + c2\ s3\ cy\ st \tag{27}$$

where si and ci are notation for sine and cosine. Equations (22)–(27) describe the readings of the accelerometers due only to the 1 G gravity vector at the point P_5 within the centrifuge which act on the pilot as he sits in the seat where the endpoint was previously defined. The next step is to calculate the linear and rotational accelerations. These accelerations produce forces and torques which act on a pilot which stress him in a physiological sense.

The derivation of the linear accelerations can now be accomplished by first expressing a vector P_5 from (X_0, Y_0, Z_0) to (X_5, Y_5, Z_5) and twice differentiating this vector. Note that if P_5 is expressed in terms of the unit vectors of the inertial frame (i_0, j_0, k_0), then by differentiating this expression, the time derivatives of the unit vectors (i_0, j_0, k_0) vanish. To determine P_5, it is composed first of a vector P_3 from (X_0, Y_0, Z_0) to (X_3, Y_3, Z_3), which can be written as:

$$P_3 = L2 i_1 \tag{28}$$

and a vector:

$$P_4 = -Lx\ i_3 + Lz\ k_3 - Ly\ j_3 + P_3 \tag{29}$$

which describes the translation from the points P_3 to P_4. Finally a vector defined by:

$$P_5 = P_4 + P_{4/5} = P_4 - Lt\ k_5 \tag{30}$$

describes the last position change to the final coordinate system. With some work (and following a procedure similar to expressing (i_5, j_5, k_5) in terms of the unit vectors of the inertial system (i_0, j_0, k_0)), the following relationships can be shown to be true:

$$i_1 = c1\ i_0 - s1\ j_0 \tag{31}$$

$$i_3 = (-s1s2c3 - c1s3)\ i_0 + (-c1s2c3 + s1s3) j_0 + (c2c3)\ k_0 \tag{32}$$

$$j_3 = (s1s2s3 - c1c3)\ i_0 + (c1s2s3 + s1c3)\ j_0 + (-c2s3)\ k_0 \tag{33}$$

$$k_3 = (-s1c2)\ i_0 + (-c1c2)\ j_0 + (-s2)\ k_0 \tag{34}$$

$$k_5 = (T_{17}^0(1,3))i_0 + (T_{17}^0(2,3))j_0 + (T_{17}^0(3,3))k_0 \tag{35}$$

where the T_{17}^0 components are defined as the orthogonal inverse of the matrix in Eq. (20). Thus expressing P_5 in terms of the inertial frame yields:

$$P_5 = (A0(t))i_0 + (B0(t))j_0 + (C0(t))k_0 \tag{36}$$

where $A0(t)$, $B0(t)$, and $C0(t)$ are written out in some detail in (Repperger, 1990). This expression can now be differentiated twice with respect to time yielding:

$$\ddot{P}_5 = (A1(t))i_0 + (B1(t))j_0 + (C1(t))k_0 \tag{37}$$

where the expressions for $A1(t)$, $B1(t)$, and $C1(t)$ are given (for completeness) in (Repperger, 1990). The next step in this procedure is to develop the rotational relationships and the Jacobian J2 of the centrifuge simulator.

Derivation of the Rotational Relationships

Determination of the Jacobian J2 for the Centrifuge: To apply these techniques for the supermaneuverability flight trajectory to a centrifuge simulator, first it is necessary to determine both the Jacobian term J2 and define the rotational trajectory of interest. At the point P_3 at the endpoint of the end effector (the point on the seat within the centrifuge), the total angular velocity of the third fixed body (the cab) can be written in vector form as:

$$\Omega = -\dot{\theta}1\ k0 + \dot{\theta}2\ k2 + \dot{\theta}3\ k3 \tag{38}$$

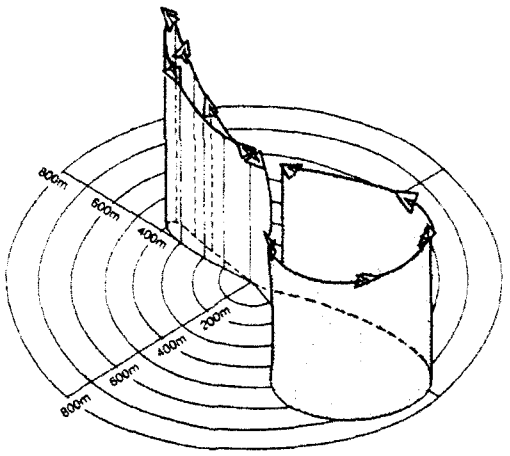

Fig. 4 The "Herbst's" maneuver—a supermaneuver

where i, j, k represent unit vectors in the coordinate systems defined in Fig. 3. It is noted that the angular velocity of the human subject within the cab is identical to the angular velocity of the cab (because the seat is fixed throughout the run). It is necessary to express $k2$ and $k3$ in terms of the inertial coordinates ($i0$, $j0$, $k0$). From the relationships derived in Table 2, it is seen that:

$$k2 = (c1)i0 - (s1)j0 \tag{39}$$

and $k3$ can be described via:

$$k3 = (-sl\ c2)i0 + (-c1\ c2)\ j0 + (-s2)\ k0 \tag{40}$$

Now substituting (39) and (40) into (38) yields for the Ω of the third rigid body to be expressed in terms of the inertial frame as:

$$\Omega = A2(t)i0 + B2(t)j0 + C2(t)k0 \tag{41}$$

where for completeness, it is seen:

$$A2(t) = \dot{\theta}2c1 - \dot{\theta}3\ s1\ c2 \tag{42}$$

$$B2(t) = -\dot{\theta}2s1 - \dot{\theta}3\ c1\ c2 \tag{43}$$

$$C2(t) = -\dot{\theta}1 - \dot{\theta}3\ s2 \tag{44}$$

To determine the Ω in the last coordinate system at the subject, Eq. (41) must be multiplied by T_8^{17} from (Repperger, 1990, 1991) to yield:

$$\Omega = A3(t)i0 + B3(t)j0 + C3(t)k0 \tag{45}$$

where it can be shown that:

$$A3(t) = \ddot{\theta}_2c1 - \dot{\theta}_2\dot{\theta}_1s1 - \ddot{\theta}_3s1c2 - \dot{\theta}_3\dot{\theta}_1c1c2 + \dot{\theta}_3\dot{\theta}_2s1s2 \tag{46}$$

$$B3(t) = -\dot{\theta}_2s1 - \dot{\theta}_2\dot{\theta}_1c1 - \ddot{\theta}_3c1c2 + \dot{\theta}_3\dot{\theta}_1s1c2 + \dot{\theta}_3\dot{\theta}_2c1s2 \tag{47}$$

$$C3(t) = -\ddot{\theta}_1 - \ddot{\theta}_3s2 - \dot{\theta}_3\dot{\theta}_2\ c2 \tag{48}$$

But recall from the definition of the J2 Jacobian term, the relationship:

$$\Omega = J2\dot{\theta} \tag{49}$$

translates into:

$$\dot{\theta} = J2^{-1}\Omega \tag{50}$$

when J2 is invertible. For simplicity to integrate Eq. (50) forward in time, a first-order Euler method will be used of the form:

$$\theta_{k+1} = \theta_k + \Delta t\dot{\theta}_k \tag{51}$$

or

$$\theta_{k+1} = \theta_k + \Delta t[J2^{-1}]\Omega(t) \tag{52}$$

where Ω is specified apriori.

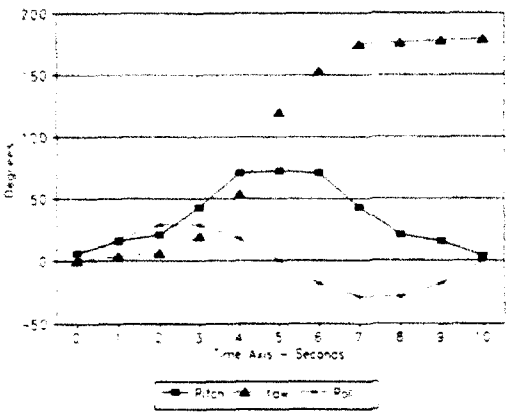

Fig. 5 An approximation for the roll, pitch, and yaw time histories with respect to the aircraft's axes when emulating the Herbst's maneuver

Application to the First Supermaneuver—The Herbst's Maneuver

This is the first classical supermaneuver that was designed from the original concept of Herbst (Herbst, 1972). However this method, it turns out, will be applied to a trajectory which produces a singular Jacobian matrix. To specify $\Omega(t)$ for the supermaneuverable trajectory called the "Herbst's Maneuver" (Herbst, 1972, 1980, 1983) as illustrated in Fig. 4, and in terms of body axis rotations of the airplane in Fig. (5), the following approximations are made for the roll, pitch, and yaw rotations (t is in units of seconds and the angles are in radians):

$$\text{Roll rotation} = \theta x(t) = .16\ \pi\ \sin\ [(\pi/5)t] \tag{53}$$

$$\text{Yaw rotation} = \theta z(t) = (\pi/180)t^3 \text{ for } 0 < t < 5 \tag{54}$$

$$= .436t \text{ for } 5 < t < 7 \tag{55}$$

$$= \pi(1 - \epsilon^{-(t-4.1)}) \text{ for } 7 < t < 10 \tag{56}$$

$$\text{Pitch rotation} = \theta y(t) = \pi(.22 - .19\ \cos\ [(\pi/5)t]) \tag{57}$$

This yields for rotational velocity space:

$$\Omega x(t) = .03\ \pi^2\ \cos[(\pi/5)\ t] \tag{58}$$

$$\Omega y(t) = .38\ \pi^2\ \sin(\pi/5)\ t \tag{59}$$

$$\Omega z(t) = \pi/60\ t^2 \text{ for } 0 < t < 5 \tag{60}$$

$$= .436 \text{ for } 5 < t < 7 \tag{61}$$

$$= \pi\epsilon^{-(t-4.1)} \text{ for } 7 < t < 10 \tag{62}$$

The matrix J2 can easily be obtained for the centrifuge from the relationship (49) by writing Ω in terms of $\dot{\theta}1$, $\dot{\theta}2$, and $\dot{\theta}3$. The terms of J2 are listed here for completeness:

J2, The Jacobian of the Centrifuge

$$J2 = \begin{pmatrix} sy\ ct, & -st\ c1 + cy\ ct\ s1, & s1\ c2\ st + c1\ c2\ cy\ ct + s2\ sy\ ct \\ -cy, & s1\ sy, & c1\ c2\ sy - cy\ s2 \\ -sy\ st, & -c1\ ct - s1\ cy\ st, & s1\ c2\ ct - c1\ c2\ cy\ st - s2\ sy\ st \end{pmatrix} \tag{63}$$

The objective is to determine an inverse kinematics solution similar to Eq. (6). A specific seat yaw rotation and seat back angle have been assumed (θy = 0 degrees, θt = 90 degrees). The Jacobian in this case represents parameters of the centrifuge simulator and is specified via:

$$J2 = \begin{pmatrix} 0, & -c1, & s1\ c2 \\ -1, & 0, & -s2 \\ 0, & -s1, & -c1\ c2 \end{pmatrix} \tag{64}$$

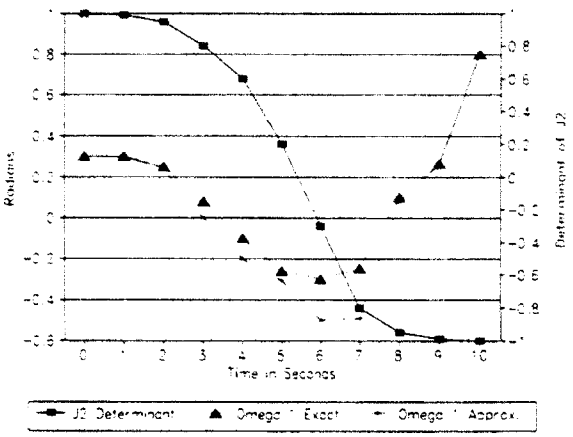

Fig. 6 Herbst's maneuver simulation

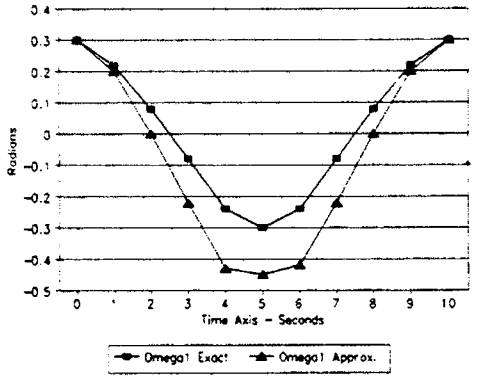

Fig. 7 Herbst's maneuver simulation using damped least squares

The $X(t)$ vector in Eq. (1) corresponding to the "Herbst's Manuever" is described in Eqs. (58)–(62) for $t \in [0, 10]$. It can be shown (Fig. 6) that the determinant of $J2$ vanishes at $t = 5.5$. Applying a Frobenious norm at $t = 5.5$ when $J2$ becomes rank deficient, it is determined that $\|\dot{X}\|^2 = 14.2$. The limits on joint velocities and torques in their appropriate dimensions requires $C \leq 1025.$, thus resulting in (at $t = 5.5$), $\|J2\|^2_{Fr} = 3.01$, even though J2 is rank deficient. Thus C in Eq. (7) constrains θ such that:

$$\|\dot{\theta}\|^2 \leq C = 1025.0 \tag{65}$$

in the appropriate joint velocity/torque dimensional units for this problem. It can easily be shown that if the selection is made:

$$\lambda = 5 \tag{66}$$

is an appropriate choice of this variable. In a least squares sense this will provide:

$$\|\dot{\theta}\|^2 \leq 1025.0 \tag{67}$$

Figure 7 illustrates this implementation for $\lambda = 5$ with the resulting decrease in the joint velocities constrained via $\|\dot{\theta}\|^2 \leq 1025.0$. Notice also the compromise in the fidelity of the motion field simulation which has to be traded off in order to limit the joint velocities and torques. Figure 6 shows an attempted solution without using damped least squares and the apparent divergence of the computed inverse kinematics algorithm at $t = 5.5$.

Application to the Second Supermaneuver—The "Cobra Maneuver"

The second trajectory selected is termed the "Cobra Maneuver." This has been demonstrated by actual aircraft in flight scenarios (*Aviation Week and Space Technology*, 1990). For this particular supermaneuver, the assumption is made for the

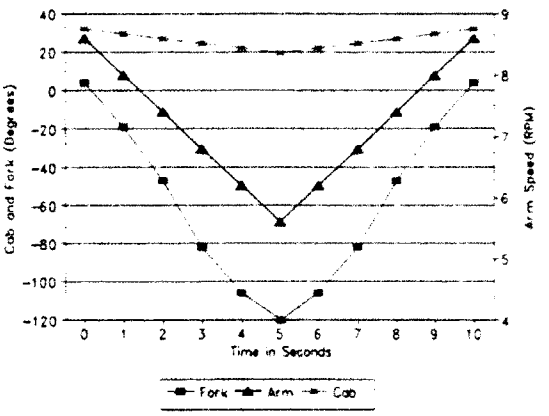

Fig. 8 Cobra simulation on centrifuge

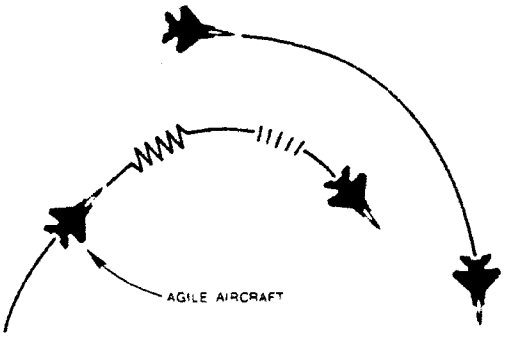

Fig. 9 Yo-yo turn for BFM (from Foltyn et al. (1987))

centrifuge simulator that $\theta_y = \pi/2$, $\theta t = 0$, and $t \in [0, 10]$ seconds. The angles are in radians. The Jacobian now becomes (for this seat configuration):

$$J2 = \begin{pmatrix} 1, & 0, & s2 \\ 0, & s1, & c1c2 \\ 0, & -c1, & s1c2 \end{pmatrix} \tag{68}$$

The Cobra Maneuver was simulated using the following angular rotations:

$$\text{Roll rotation} = \theta 3(t) = (\pi/180)(30 - 2.5t) \tag{69}$$

$$\text{Yaw rotation} = 0.0 \tag{70}$$

$$\text{Pitch rotation} = -\theta 2(t) = (\pi/3)[1 - \cos(\pi t/5)] \tag{71}$$

$$\omega 1(t) = 8.8 - .66\ t \text{ in RPM for } t \in [0, 5] \tag{72}$$

$$\omega 1(t) = 5.5 + .66\ [t - 5] \text{ for } t \in [5, 10] \tag{73}$$

It is noted that the determinant of J2 for the Cobra maneuver remained close to the value of 1.0 during this simulation and no possibility of a singular Jacobian occurred. The expression (72) for $\omega 1(t)$ is used to demonstrate the slowing down of the aircraft as it assumes its unusual attitude. In the centrifuge, the cab has to vector out to compensate for gravity which is reflected by the $\theta 3(t)$ term to compensate for the arm slowing down. Figure 8 illustrates this numerical simulation.

Application to the Third Supermaneuver—The High Yo-Yo Turn For BFM

Of the 43 supermaneuvers and 38 variations in (Foltyne et al., 1987), the third maneuver selected was the High Yo-Yo Turn for Basic Fighter Maneuver (BFM). This was chosen because this supermaneuver precludes overshoot and develops control closure (maneuver 16 of the above reference). When

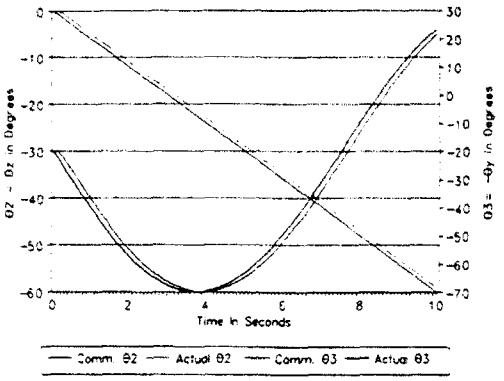

Fig. 10 Centrifuge responses to the joint commands

an aircraft flies this trajectory, it maintains controllability during the combat engagement. Figure 9 illustrates this maneuver as the agile aircraft flies this trajectory versus his opponent. For the centrifuge simulation, this is strictly a yaw and pitch motion (assuming the same seat configuration as with the Herbst's maneuver).

This motion field simulation turns out to be easier to implement than the Herbst's maneuver due to the longer time required to complete the yaw motion. Mathematically this maneuver can be characterized by the following yaw motion:

$$\theta_2(t) = \theta_z(t) = -(\pi/3)[t/10] \tag{74}$$

and the following pitch motion:

$$-\theta_3(t) = \theta_y(t) = (\pi/180)[20 + 50 \sin [2\pi\, t/15] \tag{75}$$

The determinant of the Jacobian is better behaved as compared to the Herbst's maneuver since it remains greater than zero throughout the motion trajectory. Figure 10 illustrates the commanded and actual responses of joints 2 and 3 for this supermaneuver. Finally, some comments need to be made on the inverse dynamics problems associated with these simulations.

The Issues Related to Inverse Dynamics

From observing Fig. 10, more discussion is required to describe the inverse dynamics problem in the simulation of these supermaneuverable trajectories. Space precludes an extensive discussion in this area; however, it is important to state the following facts:

(1) The arm ($\omega 1(t)$) is a velocity control system.

(2) The fork and the cab ($\theta 2(t)$ and $\theta 3(t)$) are both position control systems.

(3) Each control system was modeled somewhat independently with a disturbance input to characterize the off axes Coriolis, centrifugal, and unmodeled gravity terms.

(4) Step responses have been recorded in each axes at various arm speeds to obtain linearized models about specific operating points.

The implementation of the solution to the inverse dynamics problem can be illustrated in maneuver number 3 for the $\theta 2(t)$ response (cf. Fig. 10). Since this is a position control system, the $\theta 2$ input commands arise from the inverse kinematics solutions. The actual $\theta 2$ response of the simulator, however, differs from the $\theta 2$ input commands. A closed-loop position control system is used to drive the fork with a forward loop gain K. This closed-loop system includes the dynamics of the fork and a disturbance input to account for unmodeled effects and the undesirable Coriolis terms. The gain K is increased to reduce this position error but still must be kept small enough to maintain closed-loop system stability. There is an obvious tradeoff between stability and performance in this case and the issues related to the tradeoff between the stability of this inner loop to the resulting compromise of the fidelity of the motion field will be discussed in future papers on this topic.

References

Aviation Week and Space Technology, 1990, "British Pilot Lauds Performance of SU-27," Sept. 24, pp. 35–40.

Chiang, R. Y., M. G. Safonov, K. P. Maden, and J. A. Tekawy, 1990, "A Fixed H^∞ Controller For A Supermaneuverable Fighter Performing The Herbst's Maneuver," *Proceedings of The 1990 IEEE Conference on Decision and Control*, Dec.

Clark, G., 1987, "U.S., West German Firms Team Up To Develop Highly Maneuverable Fighter," *Defense News*, Aug. 31, p. 10.

Cook, W. J 1989, "Turning On a Dime In Midair," *US News and World Report*, Feb. 20, pp. 56–58.

Cord, T., and C. Suchomel, 1990, "Supermaneuverability," AIAA 84-2386, Nov.

Craig, J. J., 1986, *Introduction To Robotics*, Addison-Wesley Publishing Company, Inc.

Foltyn, R. W., et al., 1987, "Development of Innovative Air Combat Measures of Merit for Supermaneuverable Fighters," AFWAL-TR-87-3073, October.

Gal-Or, B., 1990, "Novel, Post-Stall, Thrust-Vectored F-15 RPVs. Laboratory and Flight Tests," First Year Report, The Jet Propulsion Laboratory, Technion, IIT.

Graettinger, T. J., and B. H. Krogh, 1988, "The Acceleration Radius: A Global Performance Measure for Robotic Manipulators," *IEEE Journal of Robotics and Automation*, Vol. 4, No. 1, 1, Feb., pp. 60–69.

Hague, D. S., 1981, "Multiple-Tactical Aircraft Combat Performance Evaluation System," *J. Aircraft*, Vol. 18, No. 7, July, pp. 513–519.

Herbst, W. B., and Krogull, B., 1972, "Design For Air Combat," AIAA Paper 72-742, AIAA 4th Aircraft Design Flight Test and Operation Meeting, Los Angeles, Calif., Aug. 7–9.

Herbst, W. B., 1980, "Future Fighter Technologies," *J. Aircraft*, Vol. 17 No. 8, Aug., pp. 561–566.

Herbst, W. B., 1983, "Dynamics of Air Combat," *AIAA Journal*, Vol. 20.

Kalviste, J., 1986, "Spherical Mapping and Analysis of Aircraft Angles for Maneuvering Flight," *Proc. of AIAA Atmospheric Flight Mechanics Conference*, Aug. 18–20, Williamsburg, VA.

Maciejewski, A., and C. A. Klein, 1988, "Numerical Filtering For the Operation of Robotic Manipulators Through Kinematically Singular Configurations," *Journal of Robotic Systems*, Vol. 5, No. 6, pp. 527–552.

Orin, D. E., and W. W. Schrader, 1984, "Efficient Computation of The Jacobian For Robot Manipulators," *The International Journal of Robotics Research*, Vol. 3, No. 4, Winter, pp. 66–75.

Repperger, D. W., 1990, "Determination of A Simulator's Capability Using Work Volume Techniques," 1990 American Automatic Control Conference, San Diego, Calif., pp. 2063–2068.

Repperger, D. W., 1991, "Matrix Continued Fraction Algorithms for Inverse Kinematics/Dynamics With Application to Simulation of Supermaneuverable Trajectories on Centrifuges," 1991 American Control Conference, Boston, Mass.

Schefter, J., 1989, "X-31- How They Are Inventing A Radical New Way To Fly," *Popular Science*, Feb., pp. 59–64.

Sweetman, B., 1990, "Fighter Agility - The 'Bruce Lee Factor,'" *International Defense Review*, Vol. 4, pp. 395–397.

Wampler, C. W., 1986, "Manipulator Inverse Kinematic Solutions Based on Vector Formulations and Damped Least Squares Methods," *IEEE Transactions on Systems, Man, and Cybernetics*, Vol. SMC-16, No. 1, Jan./Feb., pp. 93–101.